Abstract.–We determined the patterns of distribution for eggs and larvae of walleye pollock by analyzing 1,929 ichthyoplankton samples collected on 32 cruises in the western Gulf of Alaska between 1972 and 1986. The combined effects of additions of recently spawned eggs, mortality, dispersion, and advection determine the location and concentrations of eggs and larvae. The vast majority of the eggs were found in spring samples, primarily in April. Larvae were found mainly in late April and May. Eggs occurred mostly in a small area near Cape Kekurnoi in Shelikof Strait, and larvae were centered progressively to the southwest of this area as they grew and were moved by advection. By the end of May, they were usually found near the Semidi Islands. However, comparisions of larval distributions in late May showed significant interannual variations in the area of concentration and larval size.

Manuscript accepted 18 September 1989.
Fishery Bulletin, U.S. 88:133–154.

Egg and Larval Distributions of Walleye Pollock *Theragra chalcogramma* in Shelikof Strait, Gulf of Alaska

Arthur W. Kendall, Jr.
Susan J. Picquelle
Alaska Fisheries Science Center, National Marine Fisheries Service, NOAA
7600 Sand Point Way N.E., Seattle, Washington 98115-0070

Walleye pollock *Theragra chalcogramma* is the dominant gadid in the subarctic Pacific Ocean and in the Bering Sea. It is a moderate-sized (to about 70 cm standard length) pelagic or semidemersal fish that frequently occurs in large aggregations. It feeds primarily on copepods and euphausids, although fish, including its own young, enter its diet (see Lynde 1984).

Intensive multinational midwater trawl fisheries are conducted for walleye pollock in the Gulf of Alaska, the Bering Sea, and the northwest Pacific Ocean. In recent years, catches of walleye pollock have been larger by weight than those of any other single species worldwide (Sharp 1987).

Although pollock spawn intermittently year-round, most spawning occurs in spring. Walleye pollock spawn planktonic eggs that require about 2–3 weeks to hatch, depending on temperature. The planktonic larval period lasts several weeks and the transition to the juvenile stage seems to be gradual. Considerable literature is available on the early life history of walleye pollock, most of it concerning the populations in the eastern Bering Sea (Dunn and Matarese 1987).

From 1972 through 1986, the Northwest and Alaska Fisheries Center (NWAFC, recently renamed the Alaska Fisheries Science Center) conducted plankton sampling in the Gulf of Alaska, primarily in the Shelikof Strait. Based on results of the surveys before 1980, Kendall and Dunn (1985) found that walleye pollock eggs, larvae, and spawning adults were in low abundances throughout the continental shelf and upper slope of the Gulf of Alaska. In spring 1980, however, a large spawning concentration was discovered in Shelikof Strait, and subsequent sampling indicated that spawning occurred there in spring every year through 1988. No concentrations of similar magnitude have been found elsewhere in the Gulf of Alaska, although other areas have not been surveyed as intensively (E.P. Nunnallee, Alaska Fish. Sci. Cent., Natl. Mar. Fish. Serv., NOAA, 7600 Sand Point Way NE, Seattle, WA 98115-0070, pers. commun., June 1988).

The migration of spawning adults into Shelikof Strait has been monitored in most years since 1980, and has proven to be quite consistent from year to year (Nelson and Nunnallee 1987). Most spawning in the Shelikof Strait occurs in a localized area in April, as demonstrated by the occurrence of eggs in NWAFC plankton samples. The vertical distribution of walleye pollock eggs in Shelikof Strait shows that a complex pattern of interaction between stage of development and local water density determines their depth of occurrence with a substantial portion occurring below 200 m (Kendall and Kim 1989). After hatching, larvae drift in the upper water column to the southwest during a developmental period of 6–8 weeks (Kendall et al. 1987). This early-life-history pattern provides an opportunity to study the recruitment mechanisms of this population.

In this paper, we summarize data on the distribution and abundance of the eggs and larvae of walleye pollock in the Gulf of Alaska, primarily in Shelikof Strait, based on NWAFC sampling from 1972 through 1986. We present this information as a backdrop for detailed studies investigating biotic and abiotic factors that influence the annual survival of these eggs and larvae.

Methods and materials

For our studies, we examined the 32 ichthyoplankton cruises that were conducted by the NWAFC between 1972 and 1986 (Tables 1 and 2). Between 1972 and 1979, 12 such surveys were conducted in various portions of the Gulf of Alaska in all months of the year except January, August, and December (Dunn et al. 1984). Most of the 12 surveys concentrated sampling over the continental shelf southeast of Kodiak Island. Occurrences of walleye pollock eggs and larvae in the 696 tows taken on these surveys were used to investigate their relative seasonal distribution. In 1980, however, when the spring spawning of walleye pollock in Shelikof Strait was discovered, all sampling through 1986 was conducted from March through May with special emphasis in the Shelikof Strait region.

Table 1

Ichthyoplankton cruises in the Gulf of Alaska, 1972–79, with numbers of bongo net tows containing walleye pollock eggs and larvae.

Cruise	Start date	End date	No. stations	Percent occurrence Eggs	Percent occurrence Larvae
1MF79	2/13	3/11	88	3	0
4DI78	3/28	4/20	80	36	21
2KE72	4/26	5/9	67	43	36
5TK79	5/16	5/24	58	29	28
2MF78	6/19	7/9	88	1	17
1PO79	9/2	10/11	18	0	0
3MF78	9/9	9/21	24	0	0
4MF78	9/26	10/7	66	0	0
5MF78	10/19	11/1	19	5	0
4MF77	10/31	11/14	59	14	7
1WE78	10/25	11/17	86	3	0
6MF78	11/8	11/16	43	0	0
Total no. stations			696	91	76

Table 2

Ichthyoplankton cruises in Shelikof Strait, March–May, and catches of walleye pollock eggs and larvae. See Appendix 1 for calculations of mean and standard error.

				Eggs			Larvae		
Cruise	Start date	End date	No. stations	Percent occurrence	Mean no. per 10 m^2	SE	Percent occurrence	Mean no. per 10 m^2	SE
1MF81	3/12	3/20	31	81	334	148	0	0.0	0.0
1SH81	3/17	3/30	46	30	205	116	2	0.2	0.2
4CH84	3/29	3/31	39	97	177,000	39,000	8	3.9	2.2
2MF81	3/30	4/8	89	92	61,000	24,900	24	6.2	2.3
1PO85	3/30	4/13	89	86	28,800	9,020	36	141	112
1MF85	4/3	4/11	84	98	46,300	5,720	3	138	55.0
5CH84	4/4	4/8	58	95	117,000	28,100	59	311	90.3
1MF86	4/5	4/12	79	100	25,100	3,170	91	342	94.0
1DA82	4/7	4/23	39	74	11,200	6,320	33	22.9	10.7
4DI78	4/11	4/12	9	78	3,820	3,460	33	60.2	30.9
1GI86	4/12	4/16	26	35	287	250	35	115	48.2
2SH81	4/19	4/24	41	56	17,100	12,300	63	2,350	1,320
1SH84	4/20	5/4	72	57	175	46.2	64	499	129
3MF81	4/26	5/2	79	96	2,470	341	98	13,700	2,310
2KE72	4/28	4/30	12	83	5,510	3,460	83	484	463
2MF86	5/2	5/18	104	98	388	58.9	100	939	74.8
2MF85	5/3	5/11	58	79	1,330	661	71	108	37.5
5TK79	5/17	5/20	19	47	115	57.6	53	303	152
4MF81	5/20	5/24	75	89	278	37.8	100	3,070	491
1CH83	5/21	5/28	58	26	38.1	19.8	91	336	51.3
2PO85	5/22	6/2	83	37	84.2	16.5	64	58.7	9.8
2DA82	5/22	5/29	41	80	271	75.4	78	58.5	13.1
3SH81	5/23	5/28	42	33	51.5	20.3	86	1,920	466

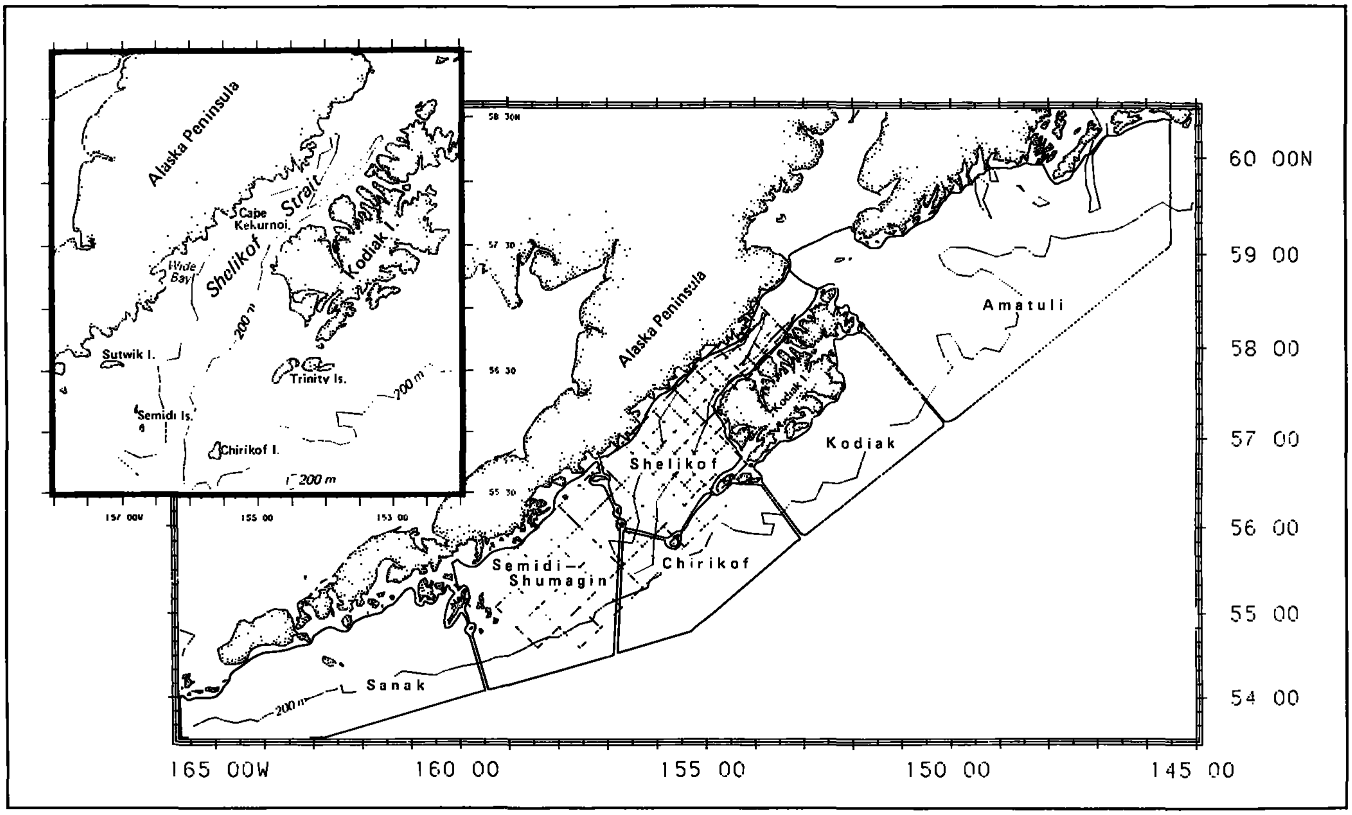

Figure 1

Gulf of Alaska showing the six strata used to analyze distribution of walleye pollock eggs and larvae. Gridded area was used in detailed analyses of the Shelikof Strait region.

The 32 cruises were conducted for a variety of purposes, so not all station patterns are ideal for the present analysis. Some results from these cruises have been reported elsewhere (Bates and Clark 1983, Dunn et al. 1984, Kendall and Dunn 1985, Bates 1987, Kendall et al. 1987). Although several ships were used, standard MARMAP oblique tows with 60-cm bongo nets (Smith and Richardson 1977) were conducted at all stations, with two exceptions: smaller bongo nets (20 cm) were used in 1984 aboard the NOAA ship *Chapman* and in April 1985 aboard the *Miller Freeman*. Mesh size was generally 505 μm, although 333-μm mesh was used aboard the NOAA Ship *Miller Freeman* in 1985 and 1986. On most cruises, sampling was conducted to a maximum depth of 200 m, as water depth permitted, but on the *Miller Freeman* in 1985 and 1986 sampling was conducted to within about 10 m of the bottom. Data collected from flowmeters in the mouth of the nets and bathykymograph records (for most tows) allowed us to determine the maximum depth and volume of water filtered for each tow. More details of the conduct of these cruises are found in Dunn and Rugen (1989).

Samples were preserved at sea in a 5% buffered formalin/seawater solution and returned to shore for processing. All fish eggs and larvae were then sorted from the samples, identified, counted, and the larvae were measured (mm standard length, SL): total sample when larvae numbered fewer than 50, or a random subsample of at least 50 when more than 50 larvae were in a sample. In each sample, developmental stages were determined for 100 randomly selected walleye pollock eggs according to the scheme of Matarese (Alaska Fish. Sci. Cent., Natl. Mar. Fish. Serv., NOAA, 7600 Sand Point Way NE, Seattle, WA 98115-0070, unpubl. manuscr.) (see Kendall and Kim 1989). Egg development data were then grouped into the six age groups used by Kendall and Kim (1989). Numbers of eggs and larvae in the tows were standardized to numbers per 10-m^2 sea surface by calculating the volume of water filtered during the tow and dividing this number by the maximum depth of the tow.

Since most tows were taken to a maximum depth of 200 m, and substantial numbers of eggs occurred below this depth, we adjusted catches of eggs, based on data in Kendall and Kim (1989), to account for eggs below

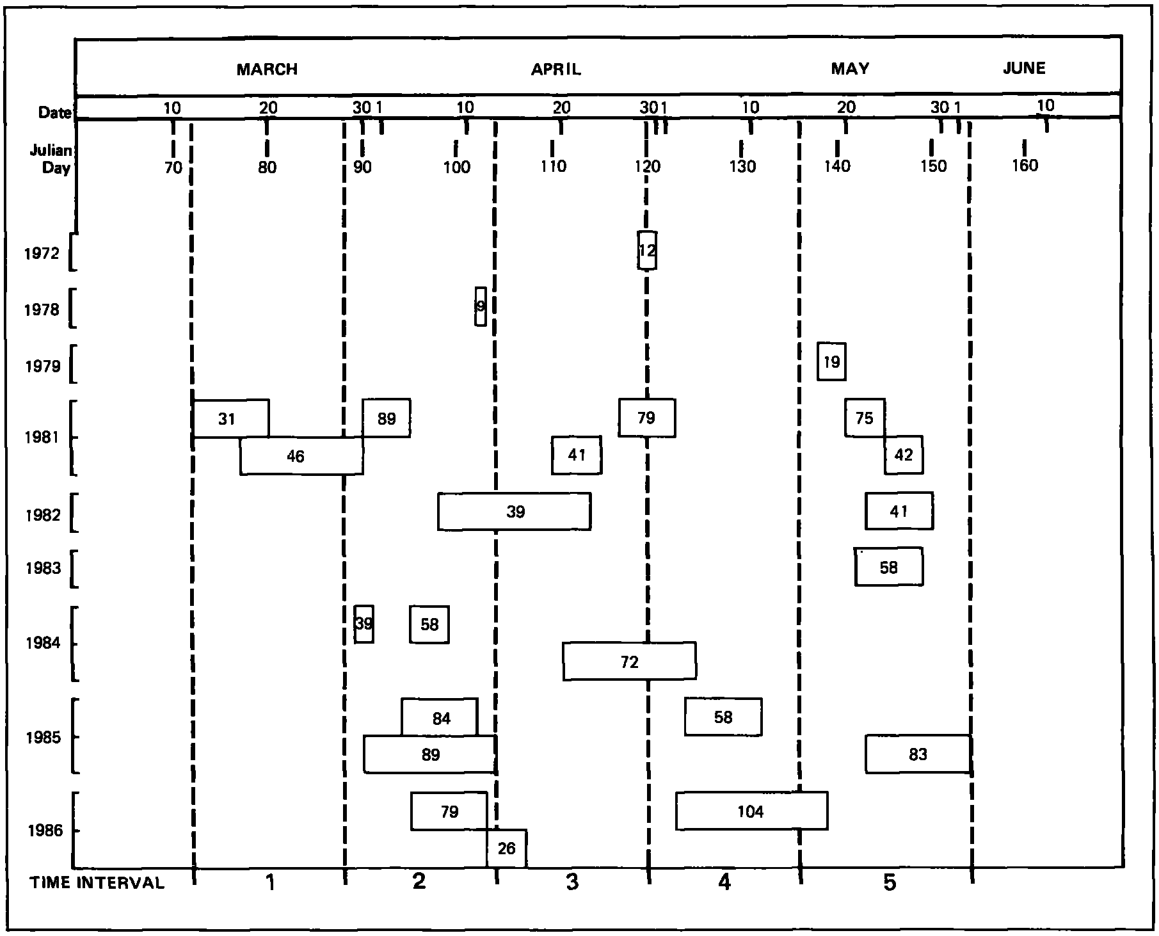

Figure 2
Cruise periods and time intervals used to analyze the distribution of walleye pollock eggs and larvae in Shelikof Strait. Numbers of tows are shown in blocks indicating cruise times.

the sampling depth. The percent of eggs that are expected to occur in the depth interval (A,B) is given by:

$$P_{A,B} = (0.06883) \cdot [\exp(0.02913 \cdot B) - \exp(0.02913 \cdot A)]$$

where $P_{A,B}$ = percent of eggs in depth interval (A,B); A = upper limit of depth interval, $\geqslant 40$ m; and B = lower limit of depth interval, $\leqslant 250$ m.

We assumed that no eggs occur at depths shallower than 40 m or deeper than 250 m. The adjustment was made by multiplying the catch per 10 m^2 by the ratio of the theoretical percentage of eggs that occur between 40 m and the bottom depth or 250 m (whichever is shallower) to the theoretical percentage of eggs that occur between 40 m and the maximum tow depth:

$$\text{Correction factor} = \frac{P_{40,\ \text{bottom depth or } 250}}{P_{40,\ \text{tow depth}}}.$$

In order to compare walleye pollock egg and larval catches at time of maximum abundance in various parts of the western Gulf of Alaska, we divided the gulf into six strata and examined egg and larval catches for each stratum (Fig. 1). For years in which more than one stratum was sampled (and at least three stations were sampled in a stratum), we used catches of eggs during April and catches of larvae from 16 May to 8 June for that year. For these cases, we calculated an area-weighted mean abundance (Sette-Ahlstrom method [see Appendix 1]) and percent contribution for each stratum.

For detailed analysis of the Shelikof Strait area, only those stations from Shelikof Strait to the Shumagin Islands were considered (see Fig. 1). Since the major spawning of walleye pollock in the western Gulf of Alaska occurs in Shelikof Strait in early spring (as we will show later), only cruises conducted in March through early June were considered in the detailed analysis of Shelikof Strait. In order to establish the general pattern of occurrence of eggs and larvae as the season progressed, this time period was divided into five intervals (12–28 March, 29 March–13 April, 14–29 April, 30 April–15 May, and 16 May–2 June), and samples collected during each interval were grouped for analysis regardless of cruise or year (Fig. 2). Intervals of a 16-18 day duration were chosen because the egg incubation period is about this duration at ambient temperatures, and larvae would grow about 3 mm in this interval (at an observed growth rate of about 0.2 mm per day [Kendall et al. 1987]). Thus eggs or larvae within a 3-mm length increment from each time interval can be considered a cohort when comparing their distribution with that of adjacent time intervals.

Similarly, since sampling patterns and positions were different for each cruise, the Shelikof Strait area was divided into a number of sectors, and the samples that were collected in each time interval and each geographic sector were grouped so they could be analyzed regardless of cruise or year. The grid of sectors was laid out with axes parallel and perpendicular to the axis of Shelikof Strait (Fig. 1). Within Shelikof Strait proper, where heaviest concentrations of stations and abundances of eggs and larvae occurred, the sectors were 10 x 10 miles (18.5 x 18.5 km); southwest of this area the sectors were 20 x 20 miles (37 x 37 km).

The geographic distributions of walleye pollock eggs and larvae were summarized by mapping their centroids of distribution (see Appendix 2). Centroids were computed for total walleye pollock eggs and larvae by time interval regardless of year, and by egg age-group and 3-mm larval length-interval (3.0–5.9, 6.0–8.9, 9.0–11.9, 12.0–14.9, 15.0–17.9 mm SL). The centroid can be considered the center of mass of the distribution and is computed as the weighted mean location of the sectors, where the weights are the estimated total number of eggs or larvae for each sector (Koslow et al. 1985):

$$\text{Centroid} = (\bar{X}, \bar{Y})$$

$$\text{where } \bar{X} = \frac{\sum_i N_i \cdot X_i}{\sum_i N_i},$$

$$\bar{Y} = \frac{\sum_i N_i \cdot Y_i}{\sum_i N_i},$$

N_i = estimated total number of pollock in sector i

$$= \frac{A_i \cdot \sum_j N_{ij}}{n_i},$$

A_i = area of sector i (in units of 10 m²)

N_{ij} = number of pollock per 10 m² for sample j in sector i,

n_i = number of samples in sector i,

X_i = center position of sector i in the east-west axis

$$= \frac{\sum_j N_{ij} \cdot X_{ij}}{\sum_j N_{ij}},$$

X_{ij} = position of sample j in sector i in the east-west axis,

Y_i = center position of sector i in the north-south axis

$$= \frac{\sum_j N_{ij} \cdot Y_{ij}}{\sum_j N_{ij}},$$

and Y_{ij} = position of sample j in sector i in the north-south axis.

The distribution was further analyzed by rotating the X and Y axes so that one axis was in the direction of the greatest geographic range of walleye pollock eggs or larvae in the study area. This axis is called the principal axis. The second axis is orthogonal to the principal axis.

An ellipse was drawn around the centroid that is one standard deviation away from the centroid along the rotated axes. The ellipse is defined as having the center at $(\bar{X}, \bar{Y})$ and the major axis parallel to the principal axis. The major and minor axes are each two standard deviations long. The ellipse is the two-dimensional analogue of a mean and standard error bars; it shows the center and the orientation of the animal's distribution in space and the amount of dispersion about the center. If the distibution of animals in space follows a bivariate normal distribution, then the ellipse is a 40% confidence contour.

Total abundance in the Shelikof Strait area was estimated for eggs and larvae for each time interval. Total abundances were also estimated for the six egg age-groups and the five larval length-increments for each time interval. The sectors were treated as strata to correct for the higher density of samples in areas of high egg and larval abundances. Not all sectors were sampled in each time interval, so the estimate of total abundance was adjusted to the total area. This was accomplished by grouping the sectors into two regions, (one included all the 10 x 10 mile sectors, and the other included all the 20 x 20 mile sectors), estimating a stratified mean density for each region, then multiply-

Table 3

Abundance of walleye pollock eggs and larvae in Shelikof Strait by time interval. Totals are expanded to total area of all sectors: ($5.556 \times 10^{10} m^2$).

Time interval	Dates	Eggs Total (10^{12})	Eggs %	Eggs SD (10^{12})	Larvae Total (10^{12})	Larvae %	Larvae SD (10^{12})	No. sectors with samples
1	12-28 Mar.	0.710	1	0.0314	<0.001	0	<0.001	48
2	29 Mar.-13 Apr.	89.6	67	10.0	0.236	1	0.0385	68
3	14-29 Apr.	38.9	29	1.69	21.1	66	2.01	64
4	30 Apr.-15 May	2.91	2	0.198	5.32	17	1.24	67
5	16 Mar.-2 June	0.681	1	0.0427	5.09	16	0.515	74

ing the density by the total area of the region (Jessen 1978).

$$N = \sum_h A_h \cdot \bar{N}_h$$

where N = estimate of total abundance,
A_h = area of region h (in units of 10 m^2)
$\bar{N}_h$ = mean density in region h (number/10 m^2)

$$= \frac{\sum_i A_{hi} \cdot \bar{N}_{hi}}{\sum_i A_{hi}},$$

A_{hi} = area of sector i in region h (in units of 10 m^2)
$\bar{N}_{hi}$ = mean density in sector i in region h (number/10 m^2)

$$= \frac{\sum_i N_{hij}}{n_{hi}},$$

N_{hij} = number/10 m^2 in sample j in sector i in region h,
and n_{hi} = number of samples in sector i in region h.

The estimate of variance was adjusted to correct for sectors with one or no sample because a minimum of two samples are required to estimate variance for each sector (see Appendix 3).

$$\hat{\text{Var}}\, N = \sum_h A_h^2 \cdot \hat{\text{Var}}\, \bar{N}_h$$

where

$$\hat{\text{Var}}\, \bar{N}_h = \frac{\sum_{i_+} A_{hi_+}^2 \cdot \hat{\text{Var}}\, \bar{N}_{hi_+}}{A_h^2} \cdot \left[1 + \frac{\sum_{i_0} A_{hi_0}^2}{\left(\sum_{i_+} A_{hi_+}\right)^2} \right]$$

i_+ refers to sectors with at least two samples,
i_0 refers to sectors with one or zero samples,

and

$$\hat{\text{Var}}\, \bar{N}_{hi_+} = \frac{\sum_j (N_{hi_+j} - \bar{N}_{hi_+})^2}{(n_{hi_+} - 1) \cdot n_{hi_+}}.$$

Results

General features of egg and larval distribution

Season of occurrence Of the 696 tows taken during the surveys from 1972 to 1979, 91 contained walleye pollock eggs and 76 contained larvae (Table 1). Between 28 March and 24 May, 205 tows were taken (29% of the total) and these included 82 and 75% of the tows containing walleye pollock eggs and larvae, respectively. A few of the tows taken between October and March also contained eggs, and the 88 tows in June and July accounted for an additional 20% of those containing larvae. From these results it appears that nearly all walleye pollock spawning and the egg and larval period in the Gulf of Alaska occurs in April and May (Table 2). Limited numbers of eggs are spawned earlier than this, and some larvae are available to plankton sampling after this.

Among the five time intervals between 12 March and 2 June established to investigate occurrences of eggs and larvae in the Shelikof Strait area, the second time interval (29 March to 13 April) accounted for 67% of the eggs, and the third time interval (14 to 29 April) accounted for 66% of the larvae (Table 3). The third time interval accounted for 29% of the eggs, and the fourth and fifth intervals accounted for 17 and 16% of the larvae, respectively. These results indicate that spawning in Shelikof Strait occurs mainly in early April, and that the larvae resulting from this spawning are present in the area in decreasing numbers into June.

Areas of occurrence Comparing the catches of walleye pollock eggs from April and larvae from 16 May to 8 June from the six strata, 89% of the eggs and 45%

Table 4

Abundance estimates ($\times 10^{10}$) of walleye pollock eggs and larvae in six strata of the western Gulf of Alaska. The top number is the number of stations sampled, and the bottom number is the number of eggs or larvae.

Year	Amatuli	Kodiak	Shelikof	Chirikof	Semidis-Shumagin	Sanak
Eggs (April)						
1981		15	104	13	16	
	[32.7]*	1.16	1670	102	1.60	[57.9]
1982		12	14	11	24	20
	[47.2]	1.24	907	99.0	21.6	48.2
1984	73	3	88	23	28	
	29.0	1.61	2240	0.510	0.744	[19.0]
1985	23	18	160	20	5	
	28.8	2.74	1220	177	0.434	[54.1]
1986	45	15	82	17	22	30
	11.3	2.47	635	13.5	13.1	88.3
Mean no. eggs	29.8	1.84	1330	78.4	7.50	53.5
Percent	1.98	0.122	88.6	5.20	0.498	3.55
Larvae (16 May–8 June)						
1979	11	13	8	9	10	7
	0.0409	0.00	38.4	0.0432	0.196	0.520
1981		11	93	13	15	
	[24.2]	0.0181	99.7	27.9	42.6	[10.4]
1982		4	15	13	23	6
	[4.80]	2.37	1.14	1.13	3.39	0.997
1985	40	3	49	23	30	29
	55.7	0.807	5.06	0.892	0.181	2.00
Mean no. larvae	21.2	0.798	36.1	7.50	11.6	3.47
Percent	26.3	0.990	44.7	9.30	14.4	4.30

*No data were available for abundance estimates in brackets; these values were predicted using a technique from analysis of variance for estimating missing data in a randomized block experiment (Cochran and Cox 1957), where the strata were considered as treatments, the years as blocks, and observed abundance estimates were log transformed.

of the larvae occurred in the Shelikof stratum (Table 4). The next most important stratum for eggs was Chirikof, where 5.2% occurred. The Amatuli stratum contained 26% of the larval catch, and the Semidis-Shumagin stratum contained 14%. Larval catches in the Amatuli stratum were based mainly on sampling done in 1985, a year in which larval occurrences in Shelikof Strait were dissimilar to all other years sampled (see later).

Distribution of eggs in Shelikof Strait

All ages Throughout the five time intervals, most sectors with high abundances of walleye pollock eggs were in Shelikof Strait proper (Fig. 3). The geographic pattern of abundance varied little among the time intervals. Most eggs were found near Cape Kekurnoi during the second time interval, although they were somewhat south of there during all other time intervals. Relatively few eggs occurred southwest of a line between Sutwik and Chirikof Islands.

The centroid for the first time interval was located off the southwest end of Kodiak Island (Fig. 4). In the second time interval, when most (67%) of the eggs were collected, the centroid was midway between Kodiak Island and the Alaska Peninsula, off Cape Kekurnoi. This is the area of maximum spawning as indicated by fishery catches and hydroacoustic surveys of adults (Alton 1987, Nelson and Nunnallee 1987). The centroid position from the first time interval is in an area where adults seem to congregate shortly before their ultimate move to the Cape Kekurnoi area. The size of the ellipses increased somewhat from the second through fifth time intervals, particularly in the along-strait direction,

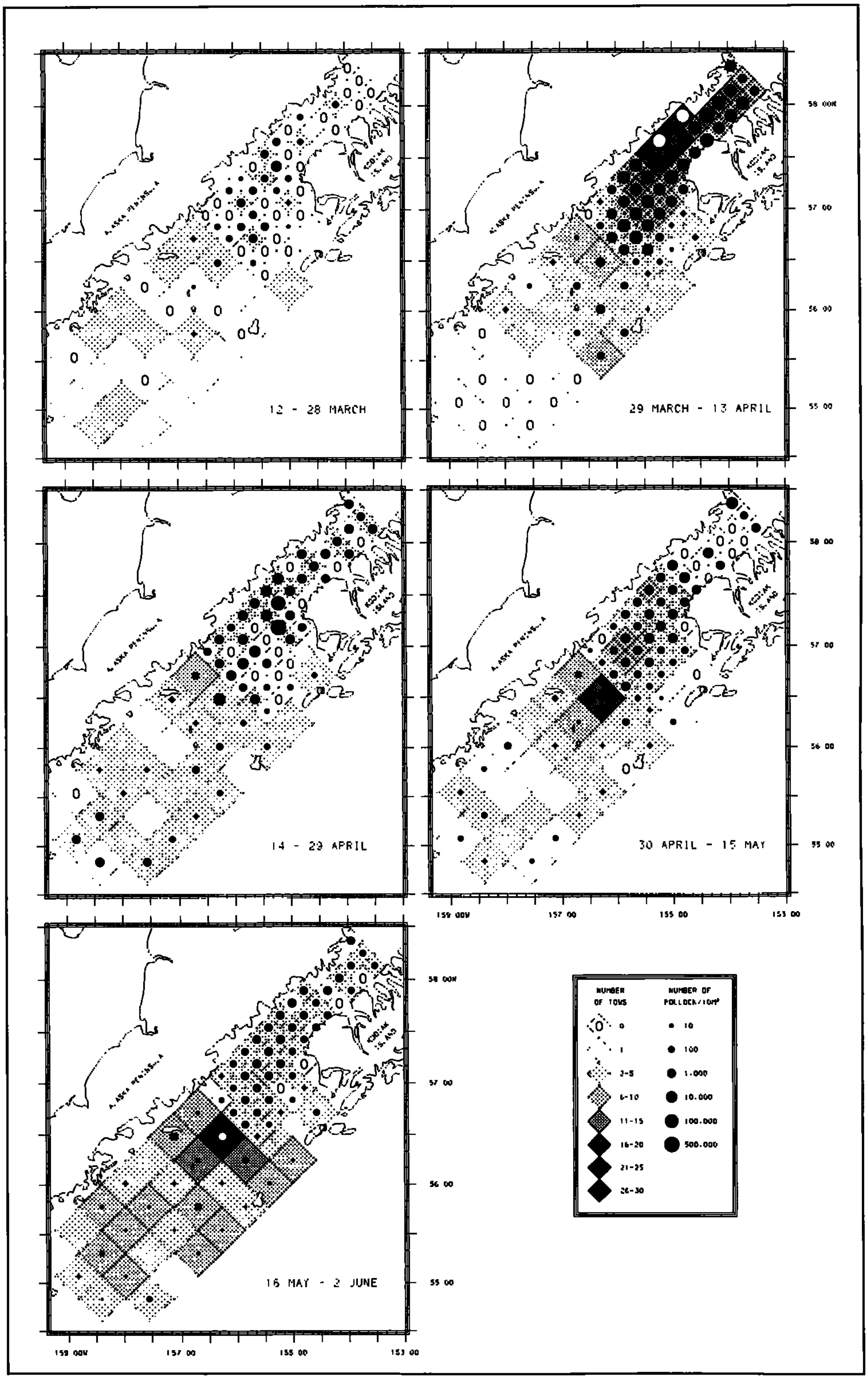

Figure 3
Distribution of walleye pollock eggs sampled in Shelikof Strait by time interval.

presumably indicating that more dispersed spawning occurs later in the season. Little change in spawning area through the season is indicated from the positions of the centroids. The centroids from the first, third, and fifth time intervals are essentially in the same location, whereas those from the second and fourth time intervals are further northeast, but in virtually the same locations. The sizes and positions of the ellipses

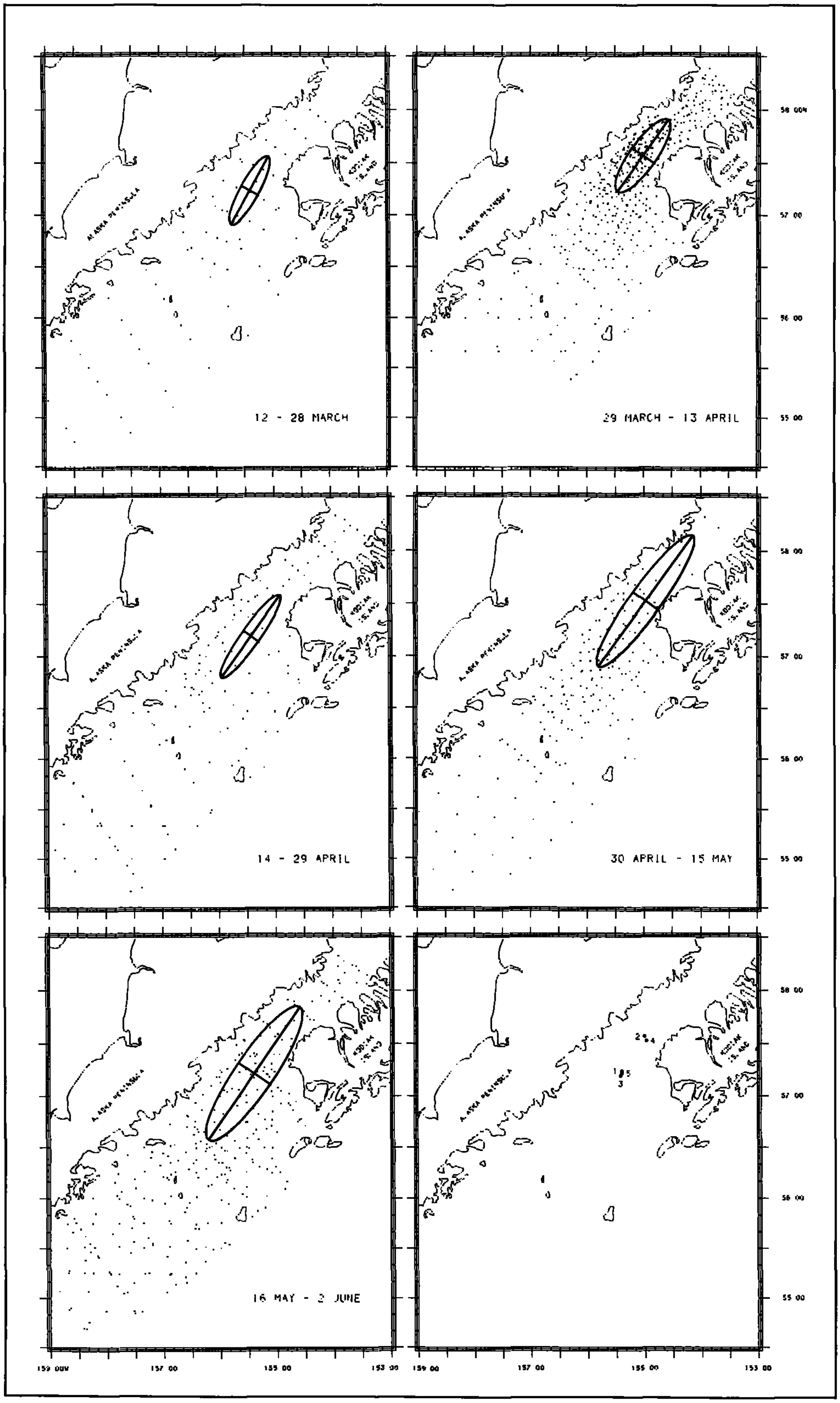

Figure 4
Centroids and associated ellipses of the distribution of walleye pollock eggs in Shelikof Strait. Dots show station locations. Lower right panel shows centroids for all five time intervals.

Table 5
Abundance of walleye pollock eggs in Shelikof Strait ($\times 10^{12}$/day) by age group and time interval. Cumulative hours to the endpoint of development of each age group at 5°C are based on Kendall and Kim (1989).

			Age group					
Time interval	Dates	Hours	1 23.0	2 70.5	3 114.5	4 166.5	5 226.5	6 316.5
1	12–28 Mar.		0.101	0.154	0.0558	0.0255	0.0152	0.0302
2	29 Mar.–13 Apr.		20.4	11.8	12.4	4.62	4.34	0.828
3	14–29 Apr.		1.23	3.07	2.75	1.93	4.75	2.81
4	30 Apr.–15 May		0.331	0.252	0.253	0.225	0.204	0.168
5	16 May–2 June		0.0502	0.0577	0.0636	0.0408	0.0503	0.0502

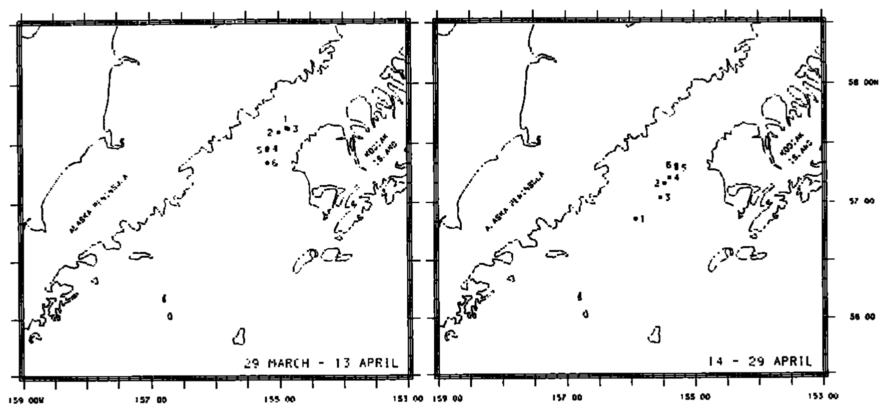

Figure 5
Centroids of walleye pollock egg distributions in Shelikof Strait by age group (see Table 5) during time intervals 2 (29 Mar.–13 Apr.) and 3 (14–29 Apr.).

reflect the extent of intra- and interannual variations in geographic patterns of distribution; and since the ellipses overlap each other, it appears that there is little variation in occurrences of the eggs through the season or among years. It should be noted, however, that the first time interval was sampled only in 1981; at least 5 years were sampled for all other time intervals.

By age group The trend in abundances over the various age groups of eggs varies with the time interval (Table 5). The young ages (groups 1–3) are much more abundant than the older ages (groups 4–6) in time intervals 1 and 2. This is due to the combined effects of mortality reducing the number of older eggs, and an increasing spawning rate producing young eggs at a higher rate than the older eggs were produced. During time intervals 3, 4, and 5, the abundances of young and old eggs are nearly equal. This is probably due to a declining spawning rate producing fewer young eggs; additionally the mortality rate might be lower than during time intervals 1 and 2.

Centroids of eggs by age group for the five time intervals indicated that in most cases random events and sampling error may have masked patterns of changes in spawning distribution and advection and dispersion of the eggs. The ellipses around the centroids of the six age groups generally overlapped one other within a time interval. It appears that distribution of spawning has more influence on distribution of eggs than advection, even though the eggs have a 2-week incubation period. Only the centroids of the six age groups of eggs for the second and third time intervals, when most eggs occurred, were analyzed (Fig. 5). The locations of centroids from the second time interval show that eggs in age groups 4–6 are close to one other and located south of eggs in age groups 1–3. This demonstrates that spawning during this interval may occur in two distinct but nearby areas. Spawning in the southern area would take place earlier than in the northern area, as indicated by the location of the centroid of all egg ages from the first time interval (Fig. 4). During the third time interval, the distribution of ages is the opposite of the pattern seen in the second time interval, with the older eggs located to the north of the younger eggs. This pattern indicates that the spawning adults were moving to the south during this time interval.

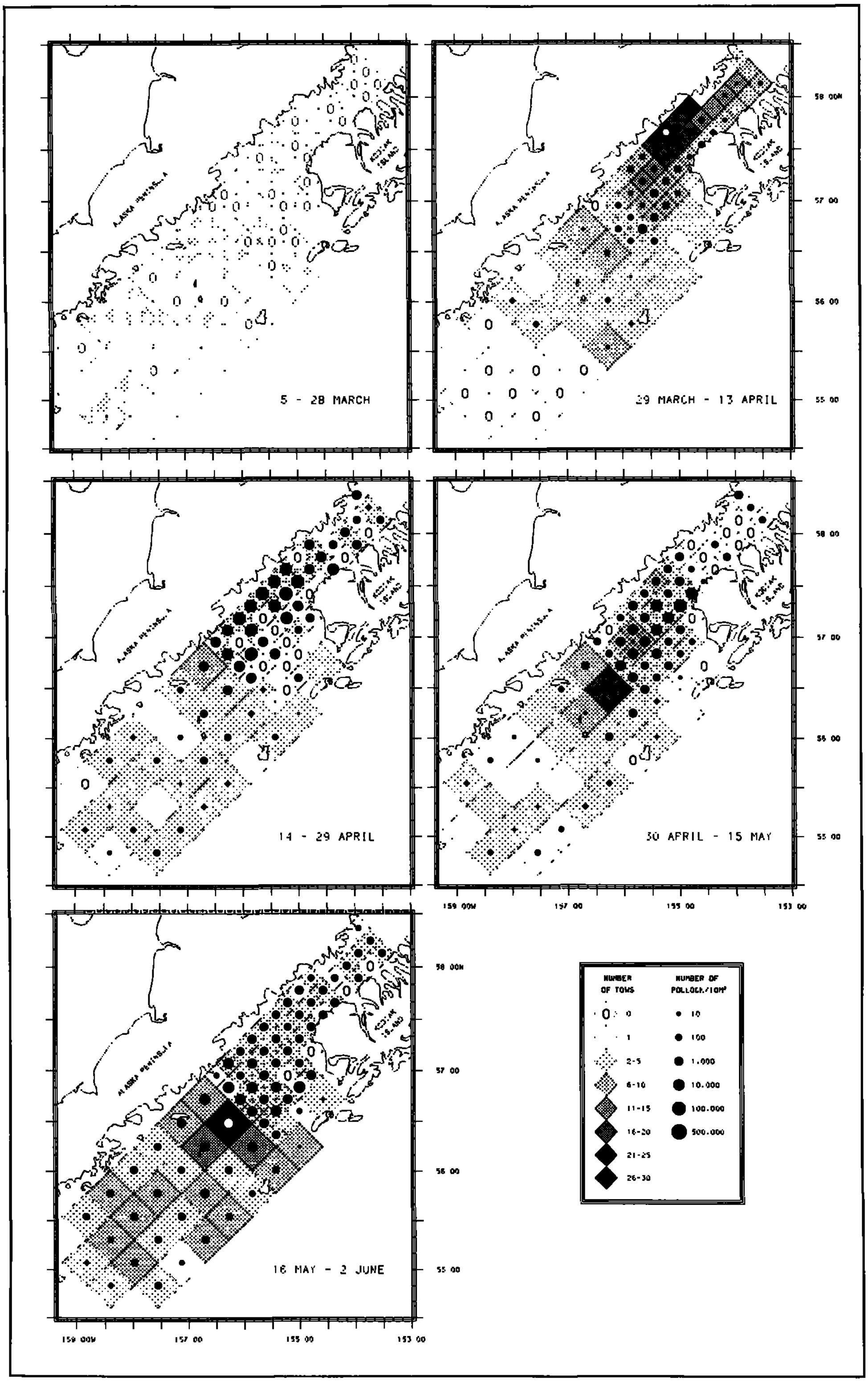

Figure 6
Distribution of walleye pollock larvae sampled in Shelikof Strait by time interval.

Distribution of larvae in Shelikof Strait

All lengths A single walleye pollock larva was found in the southwest corner of the study area during the first time interval (Fig. 6). By the second time interval, low numbers of larvae were found in most sectors in Shelikof Strait proper. Toward the southern end of the strait, they were mainly in the center of the strait, over the deep trough. A few sectors southwest of a line

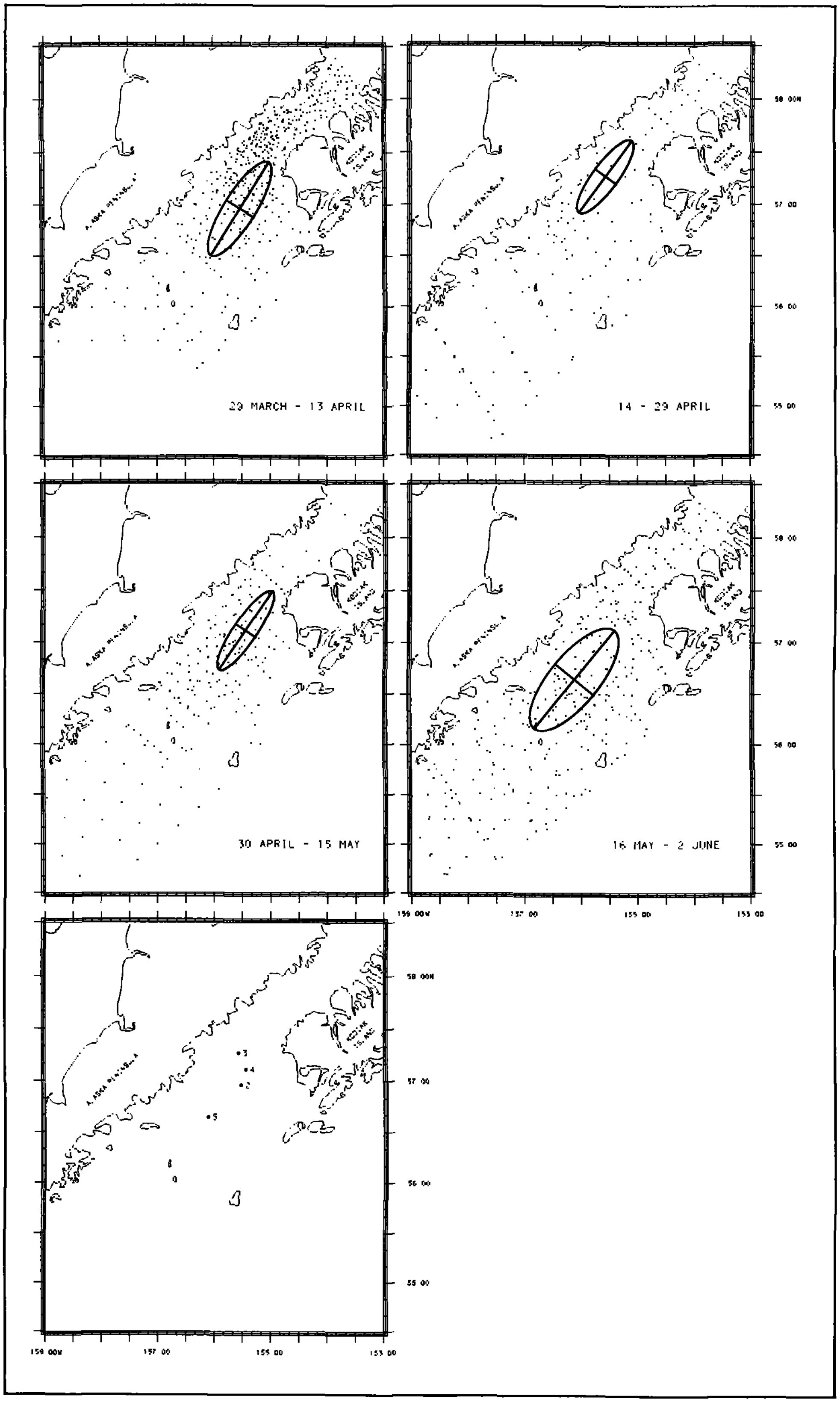

Figure 7
Centroids and associated ellipses of the distribution of walleye pollock larvae in Shelikof Strait. Dots show station locations. Lower panel shows centroids for second through fifth time intervals.

between Sutwik and Chirikof Islands had a few larvae. During the third time interval most sectors in Shelikof Strait proper contained large numbers of larvae. The larvae seemed to be most abundant along the Alaska Peninsula. South of Sutwik Island, most of the sectors contained a few larvae, with most larvae tending to occur in sectors along the deep trough and along the continental shelf margin. In the fourth time interval larvae were mainly in lower Shelikof Strait south to Chirikof Island. They were more abundant in the center of the strait over the deep trough than along the Alaska Peninsula. Larvae were present in nearly all sectors during the fifth time interval, and they were more widespread and relatively more abundant south of Sutwik Island than previously. Sectors with highest concentrations of larvae were between the south end of Kodiak Island and Chirikof Island.

Centroids of the larval distributions by time interval represent the results of spawning locations and advection and mortality of the eggs and larvae (Fig. 7). During the second time interval, the centroid of the larval distribution was over the deep trough between the Trinity Islands and the Alaska Peninsula, slightly south of the centroid of eggs during the previous time interval. The location of this larval centroid probably largely reflects advection of larvae from the eggs sampled in the previous time interval. These few larvae are not apparent in later time intervals, probably because their numbers are overwhelmed by larvae produced from the more intense later spawning near Cape Kekurnoi. The centroid of larvae during the third time interval was in the center of the strait between Cape Kekurnoi and Wide Bay. This is north of the larval centroid, but southwest of the egg centroid, from the previous time interval. Samples from the second time interval accounted for most of the eggs, whereas samples from the third time interval accounted for most of the larvae. The larvae collected in the third time interval primarily resulted from the eggs observed in the second time interval. The difference in location of the egg centroid from the second time interval and the larval centroid from the third time interval is probably largely due to advection to the southwest of eggs and larvae between these intervals. The larval centroid from the fourth time interval was displaced slightly to the south of the larval centroid from the third time interval. The sizes of the ellipses from these two time intervals were essentially equal, indicating that physical diffusive processes were balanced by biological processes of recruitment and mortality and physical processes counteracting dispersal. The larval centroid from the fifth time interval was displaced to the southwest from that of the fourth time interval, and the ellipse was considerably larger. The shape of the ellipse indicated that the larvae were more dispersed in both the along- and across-strait directions than previously. Based on the low numbers of eggs collected after the second time interval, the larval centroids from the fourth and fifth time intervals largely reflect displacement of eggs and larvae first seen as eggs during the second time interval.

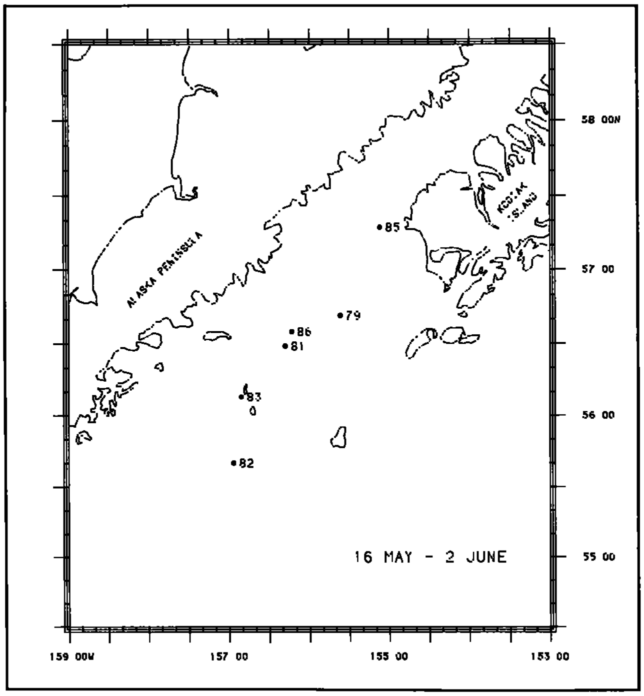

Figure 8
Centroids of walleye pollock larval distributions in Shelikof Strait during the fifth time interval (16 May–2 June), 1979–86.

Interval 5 by year The fifth time interval evinced considerable variation in the location of the larval centroids among the years sampled (Fig. 8). The centroid of larvae in 1985 was off the westernmost coast of Kodiak Island. The ellipse from 1985 was quite elongate in its along-strait axis due to the occurrence of larvae further north in Shelikof Strait than seen in any other year sampled. The centroids from 1979, 1981, and 1986 were close to one another over the trough between Sutwik and Chirikof Islands. In 1983, the centroid was in the Semidi Islands, and in 1982 it was further south, between Chirikof Island and the Alaska Peninsula. The centroid from 1985 was 290 km northeast of the centroid from 1982.

Larval lengths A plot of weighted mean length of larvae versus weighted mean sampling date* for each

*Weighted mean sampling date = $\bar{D}$, where

$$\bar{D} = \frac{\sum_i N_i \cdot D_i}{\sum_i N_i}.$$

N_i = number/10 m^2 in sample i, and
D_i = day of year when sample i was taken.

cruise permits a comparison among years, and provides an estimate of the increase in length of fish in the population with time (Fig. 9). The mean length of larvae in the population at a particular time results from a combination of time since spawning and individual growth, as well as the effects of mortality. Older larvae will have been subjected to mortality for longer periods than younger larvae, so the change in length of larvae in the population should be less than individual growth rate. In 1978, 1979, and 1983, only one cruise sampled larvae. However, in 1981 and 1985, five and four cruises, respectively, sampled larvae. Altogether, 20 cruises were available to assess larval-population length increase.

Before the third time interval, little increase in the length of larvae in the population or variation among years in size of larvae was evident. The mean lengths were 3–6 mm. Larvae at the end of April were smallest in 1981 and largest in 1985. After the middle of May, the larval population length seemed to increase at a fairly uniform and linear rate through the end of May. In 1981, 1982, and 1985, larvae in late May were between 7 and 9 mm. In 1983, however, larvae were over 10 mm in late May. Excluding the larval lengths from 1983, the length data from the third through fifth time intervals fit the straight line of

$$\text{length (mm SL)} = -9.60 + 0.122 \cdot \text{day of year},$$

with $r^2 = 89.7$. Thus the population increased in length at a rate of about 0.12 mm/day. Based on analysis of larval otolith daily growth increments, individual growth in 1983 was 0.2 mm/day (Kendall et al. 1987).

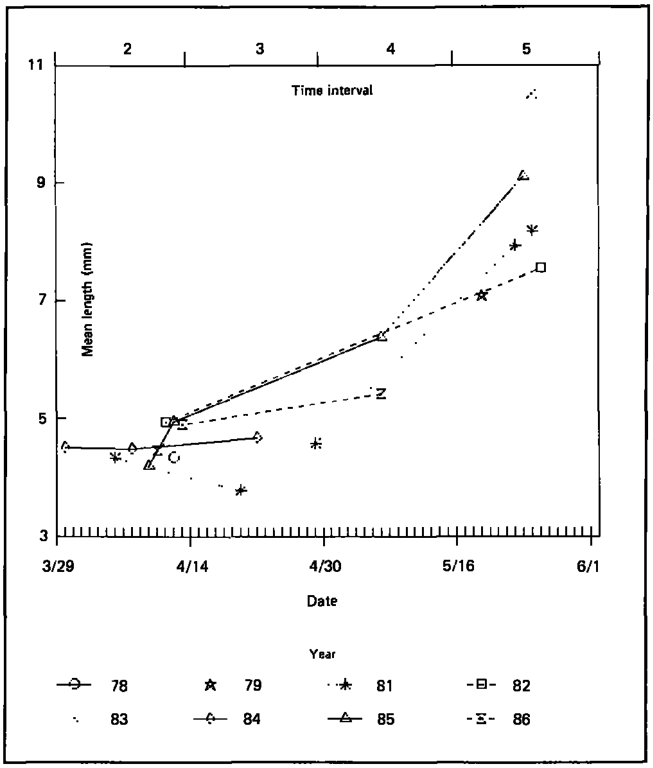

Figure 9
Lengths of walleye pollock larvae by sampling date and year.

Distribution of cohorts of eggs and larvae in Shelikof Strait

The five time intervals of 16–18 days were about equal to the incubation period of the eggs, and the larvae grew about 3 mm (~0.17 mm/day) during each time interval, after hatching at 3–4 mm. Thus eggs from one time interval were assumed to be the 3–6 mm larvae observed in the following time interval, the 6–9 mm larvae in the time interval after that, and so on. Under this assumption three cohorts (1–3) were established, based on eggs from the first, second, and third time intervals, regardless of year, in order to examine the geographic displacement of the eggs and larvae during development (Table 6). Changes in abundance with time in the cohorts is influenced by differences among years in sampling and overall population abundances, which prevent estimation of mortality rates.

Eggs in the first cohort, those from the first time interval, were slightly northeast of larvae in this cohort, which were represented by 3–6 mm larvae from the second time interval (Fig. 10). The centroid of larvae that were 3–6 mm long in the second time interval was in the southern end of Shelikof Strait, midway between the southern end of Kodiak Island and the Alaska Peninsula. In the third time interval the first cohort (6–9 mm larvae) was centered further to the southwest, just north of a line between Sutwik and Chirikof Islands. In the fourth time interval the 9–12 mm larvae were centered near the position of the centroid of the 3–6 mm larvae in the second time interval. The ellipse for these larvae was quite elongate (Table 6), indicating considerable dispersion on the along-strait axis. This pattern reflects differences in the distribution of this size larvae among years, particularly in the abundance of these larvae in the northern part of Shelikof Strait in 1985. The centroid of the 12–15 mm larvae from the fifth time interval is positioned in the Semidi Islands, and the ellipse is broadened in the across-strait dimension compared with the previous ones. Thus, excluding the fourth time interval, which was influenced by the aberrant pattern of 1985, the first cohort of eggs and larvae appears to have been advected to the southwest in the center of the strait from the southern end of Kodiak Island to the Semidi Islands between early April and late May.

Table 6

Abundance ($\times 10^{12}$) and dimensions of ellipses (of three cohorts) of walleye pollock eggs and larvae in Shelikof Strait by time interval and 3-mm length increment for larvae. Cohorts are indicated by the diagonal numbered boxes. Areas in km^2; axes in km.

Time interval	Dates		Cohort	Eggs	Larvae: Length increments (mm SL) 3–6	6–9	9–12	12–15	15–18
			1						
1	12–28 Mar.	Abundance		0.710	<0.001	0.000	0.000	0.000	0.000
		Area		1340					
		Major axis		83					
		Minor axis		21					
			2						
2	29 Mar.–13 Apr.	Abundance		89.6	0.231	0.004	0.000	0.000	0.000
		Area		2080	3400				
		Major axis		93	132				
		Minor axis		28	33				
			3						
3	14–29 Apr.	Abundance		38.9	19.7	0.204	0.001	0.000	0.000
		Area		1710	2440	1570			
		Major axis		108	104	95			
		Minor axis		20	30	21			
4	30 Apr.–15 May	Abundance		2.91	4.79	0.512	0.012	0.000	0.000
		Area			2030	4920	6310		
		Major axis			108	160	230		
		Minor axis			24	39	35		
5	16 May–2 June	Abundance		0.681	0.275	3.40	1.27	0.137	0.004
		Area				4780	9220	8910	
		Major axis				117	183	166	
		Minor axis				52	64	68	

The second cohort, represented by eggs from the second time interval and 3–6 mm larvae from the third time interval, resulted from the period of heaviest spawning activity. Most of the eggs and larvae collected were in this cohort. The centroid of the eggs of this cohort, in the second time interval, was in the middle of Shelikof Strait, off Cape Kekurnoi (Fig. 10). During the third time interval, the centroid of larvae of the second cohort (3–6 mm long) was located east of Wide Bay, southwest of the centroid of eggs of this cohort. In the fourth time interval, 6–9 mm larvae were further to the southwest, off the south end of Kodiak Island. By the fifth time interval, 9–12 mm larvae were near a line between Sutwik and Chirikof Islands. The ellipses for this cohort of eggs and larvae expanded between each successive time interval (Table 6).

The centroid of eggs of the third cohort was found in the center of Shelikof Strait, off Wide Bay (Fig. 10). The centroid of this cohort as 3–6 mm larvae (during the fourth time interval) was positioned at the southern end of Shelikof Strait, closer to Kodiak Island than to the Alaska Peninsula which was slightly south of where the eggs were. In the fifth time interval the centroid of this cohort as 6–9 mm larvae was between Sutwik Island and the Trinity Islands.

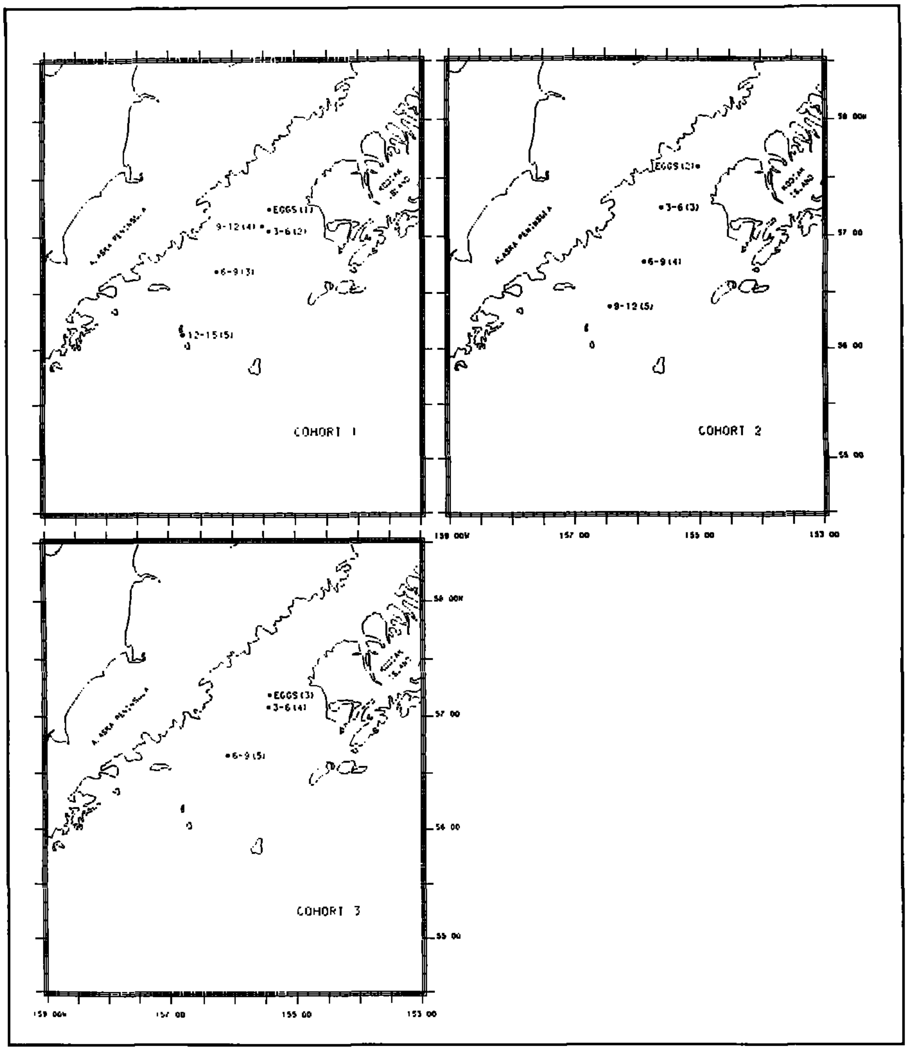

Figure 10
Centroids of three cohorts of walleye pollock egg and larval distributions in Shelikof Strait. Labels beside dots indicate stage (egg) or length increment, with time interval in parentheses.

Discussion

As we compiled data for analysis, we made several assumptions which may have affected our results. Most of the tows used to describe egg distributions did not exceed a maximum depth of 200 m and, therefore, a correction factor was applied to account for eggs in deeper parts of the water column. Our key assumption for this correction was that the depth distribution of eggs found in Shelikof Strait in 1985 and 1986 was applicable throughout the study area and for all years examined. The validity of this assumption needs to be verified by determining geographic and interannual variability in depth distribution and bouyancy of eggs. Specific gravity and depth distribution of the eggs change with development (Kendall and Kim 1989), but these changes were not accounted for in our analysis.

In many of the analyses, there was an implicit assumption that samples were drawn randomly from within a sector or stratum. Some of what appears to be random variability in the data may be features of distribution on a scale too fine for our analyses. In combining data from various years with slightly different sampling times and station patterns, small-scale interannual differences may have been blended. Effects of different sampling intensities among the years may have interacted with changes in overall abundance of eggs and larvae, so that patterns in low adundance years may have been overwhelmed by patterns from high abundance years. However, aside from the unusual spatial distribution of larvae in 1985, and the large size of larvae in late May 1983, timing and geographic areas of occurrence of eggs and larvae seemed quite consistent among years.

Knowledge of the distribution of eggs and larvae of walleye pollock in the Gulf of Alaska has increased dramatically in recent years. The larvae could not be separated from those of Pacific cod *Gadus macrocephalus* prior to studies of Matarese et al. (1981). Kendall and Dunn (1985) summarized knowledge of ichthyoplankton, including walleye pollock in the Gulf of Alaska based on sampling prior to 1980. Very little sampling had been done before 1977, when a series of cruises was conducted mainly southeast of Kodiak Island. Eggs were found mainly nearshore in spring, and to a lesser extent in fall. Larvae were found in spring and summer throughout the shelf and slope area sampled. The spawning concentration in the Shelikof Strait was discovered inadvertantly in 1980. The mean number of eggs and larvae per 10 m^2 in cruises reported by Kendall and Dunn (1985) did not exceed 40 and 228 respectively, whereas we found mean numbers per cruise as high as 177,000 for eggs and 13,700 larvae in Shelikof Strait (Table 2).

Based on the patterns of distribution elucidated here, several topics for future work are indicated. By comparing distributions of cohorts of eggs and larvae, we inferred advection rates and directions. The reasonableness of these drift patterns needs to be investigated based on the physical oceanography of the area.

Although these results show that most spawning occurs in Shelikof Strait, evidence of some spawning south of Chirikof Island was observed. Surveys of adults producing the eggs in this area need to be conducted so that the importance of the area can be evaluated. The source of the eggs and larvae found in the Amatuli area and the northern part of Shelikof Strait in 1985 also needs to be established.

The cruises available for this study were made only through early June. By this time the larvae had drifted a considerable distance southwest of the spawning area and grown to about 8–11 mm. The distribution of larvae later in spring and summer is virtually unknown. To understand recruitment in this population, the larvae need to be followed through summer to find the location of their nursery area. Such information is a necessary prerequisite to studies of factors contributing to survival throughout the planktonic stages of walleye pollock.

During the years of study here, the adult spawning biomass of walleye pollock in Shelikof Strait declined from $3.77 \cdot 10^6$ mt in 1981 to $0.62 \cdot 10^6$ mt in 1986 (Nelson and Nunnallee 1987). The planktonic egg data from these years can be analyzed to see how closely they reflect this decrease in spawning biomass. Based on the analysis here, a model of seasonal and geographic egg production could be developed that would allow extrapolation of expected egg catches when sampling did not cover the entire area of their occurrences.

Given the interannually consistent patterns of egg distribution in Shelikof Strait described here, there is a reasonable opportunity to establish egg and larval mortality rates based on changes in population abundance during April and May. The timing of changes in mortality could be determined, and differences in mortality rates among years could be investigated. This can lead to studies of the environmental and biological causes of mortality and how these vary during the season and interannually. Knowledge of these variations in mortality rates is critical to an understanding of recruitment patterns in this population.

Summary

Based on analysis of walleye pollock egg and larval distributions in 1,929 MARMAP bongo tows taken on 32 cruises in the northern Gulf of Alaska from 1972 to 1986, we made the following conclusions:

1. Most eggs occur in April, and larvae occur in late April through May.
2. Most eggs and larvae result from spawning in Shelikof Strait near Cape Kekurnoi.
3. Little difference in geographic distribution of eggs was seen through the season or among the years sampled.
4. Larvae occurred progressively to the southwest of the area of egg occurrence, as the larvae developed through the season.
5. Larval population averaged from 4.2 to 4.9 mm in mid April, and reached 7.5 to 9.1 mm by the end of May, except in 1983 when the population averaged 10.5 mm at the end of May.
6. Considerable variation in distribution of larvae was seen by late May among the years sampled, indicating differences in amount of advection.

Acknowledgments

Sample collection and processing, as well as the data entry and editing that went into producing this publication, required contributions of persons too numerous to mention; however, without them we could not have considered undertaking this project. Suffice it to say that the environment that walleye pollock find suitable for spawning is often extremely inhospitable to those on ships collecting their eggs and larvae, and we appreciate the efforts of all involved. Most samples were sorted and fish eggs and larvae identified, counted, and staged (eggs) or measured (larvae) at the Polish Plankton Sorting Center under the direction of Dr. Leonard Ejsymont, whose diligence in overcoming the many problems associated with such demanding work, as well as the challenges of a cooperative program between two countries, is gratefully acknowledged. Many people at NWAFC assisted in processing egg and larval samples, but we particularly want to thank Ann Matarese, Beverly Vinter, and Deborah Blood. Jay Clark and Richard Bates at NWAFC made the data required ready for analysis and Bates performed some of the analyses. Dr. Suam Kim, University of Washington and NWAFC, advised us on depth adjustments of egg catches and on the use of centroids for our analysis. Dr. Paul Smith, Southwest Fisheries Center, and Dr. Don Gunderson, University of Washington, reviewed and made valuable comments on an earlier draft.

Citations

Alton, M.S.
1987 Walleye pollock fishery in the Gulf of Alaska, 1985–86. *In* Major, R.L. (ed.), Condition of groundfish resources of the Gulf of Alaska region as assessed in 1986, p. 1–13. NOAA Tech. Memo. NMFS-F/NWC-119, Northwest and Alaska Fish. Cent., Natl. Mar. Fish. Serv., Seattle, WA 98115-0070.

Bates, R.D.
1987 Ichthyoplankton of the Gulf of Alaska near Kodiak Island, April–May 1984. NWAFC Proc. Rep. 87-11, Northwest and Alaska Fish. Cent., Natl. Mar. Fish. Serv., NOAA, Seattle, WA 98115-0070, 53 p.

Bates, R.D., and J. Clark
1983 Ichthyoplankton off Kodiak Island and the Alaskan Peninsula during spring 1981. NWAFC Proc. Rep. 83-09, Northwest and Alaska Fish. Cent., Natl. Mar. Fish. Serv., NOAA, Seattle, WA 98115-0070, 105 p.

Cochran, W.G., and G.M. Cox
1957 Experimental designs, 2nd ed. John Wiley & Sons, NY, 611 p.

Dunn, J.R., and A.C. Matarese
1987 A review of the early life history of northeast Pacific gadoid fishes. Fish. Res. 5:163–184.

Dunn, J.R., and W. Rugen
1989 A catalog of Northwest and Alaska Fisheries Center ichthyoplankton cruises 1965–1988. NWAFC Proc. Rep. 86-08, Northwest and Alaska Fish. Cent., Natl. Mar. Fish. Serv., NOAA, Seattle, WA 98115-0070, 78 p, 85 figs.

Dunn, J.R., A.W. Kendall, Jr., and R.D. Bates
1984 Distribution and abundance patterns of eggs and larvae of walleye pollock (*Theragra chalcogramma*) in the western Gulf of Alaska. NWAFC Proc. Rep. 84-10, Northwest and Alaska Fish. Cent., Natl. Mar. Fish. Serv., NOAA, Seattle, WA 98115-0070, 66 p.

Jessen, R.J.
1978 Statistical survey techniques. John Wiley & Sons, NY, 520 p.

Kendall, A.W. Jr., and J.R. Dunn
1985 Ichthyoplankton of the continental shelf near Kodiak Island, Alaska. NOAA Tech. Rep. NMFS 20, Natl. Oceanic Atmos. Admin., Natl. Mar. Fish. Serv., Seattle, WA 98115-0070, 89 p.

Kendall, A.W. Jr., and S. Kim
1989 Buoyancy of walleye pollock (*Theragra chalcogramma*) eggs in relation to water properties and movement in Shelikof Strait, Gulf of Alaska. *In* Beamish, R.J., and G.A. McFarlane (eds.), Effects of ocean variability on recruitment and an evaluation of parameters used in stock assessment models, p. 169–180. Can. Spec. Publ. Fish. Aquat. Sci. 108.

Kendall, A.W. Jr., M.E. Clarke, M.M. Yoklavich, and G.W. Boehlert
1987 Distribution, feeding, and growth of larval walleye pollock, *Theragra chalcogramma*, from Shelikof Strait, Gulf of Alaska. Fish. Bull., U.S. 85:499–521.

Koslow, J.A., S. Branlt, J. Dugas, and F. Page
1985 Anatomy of an apparent year-class failure: the early life history of the 1983 Browns Bank haddock *Melanogrammus aeglefinus*. Trans. Am. Fish. Soc. 114:478–489.

Lynde, C.M.
1984 Juvenile and adult walleye pollock of the eastern Bering Sea: literature review and results of ecosystem workshop. *In* Ito, D.H. (ed.), Proceedings of the workshop on walleye pollock and its ecosystem in the eastern Bering Sea, p. 43–108. NOAA Tech. Memo. NMFS-F/NWC-62, Northwest Alaska Fish. Cent., Natl. Mar. Fish. Serv., Seattle, WA 98115-0070.

Matarese, A.C., S.L. Richardson, and J.R. Dunn
1981 Larval development of Pacific tomcod, *Microgadus proximus*, in the northeast Pacific Ocean with comparative notes on larvae of walleye pollock, *Theragra chalcogramma* and Pacific cod, *Gadus macrocephalus* (Gadidae). Fish. Bull., U.S., 78:923–940.

Nelson, M.O., and E.P. Nunnallee
1987 Results of acoustic-trawl surveys for walleye pollock in the Gulf of Alaska in 1986. *In* Major, R.L. (ed.), Condition of groundfish resources of the Gulf of Alaska region as assessed in 1986, p. 15–38. NOAA Tech. Memo. NMFS-F/NWC-119, Northwest Alaska Fish. Cent., Natl. Mar. Fish. Serv., Seattle, WA 98115-0700.

Richardson, S.L.
1981 Spawning biomass and early life of northern anchovy, *Engraulis mordax*, in the northern subpopulation off Oregon and Washington. Fish. Bull., U.S. 78:855–876.

Sharp, G.D.
1987 Climate and fisheries: cause and effect or managing the long and short of it all. *In* Payne, A.I.L., et al. (eds.), The Benguela and comparable ecosystems. S. Afr. J. Mar. Sci. 5:811–838.

Shuster, J.J.
1982 Nonparametric optimality of the sample mean and sample variance. Am. Stat. 36:176–178.

Smith, P., and S. Richardson
1977 Standard techniques for pelagic fish egg and larva surveys. FAO Tech. Publ. 75, 100 p.

Sokal, R.R., and F.J. Rohlf
1981 Biometry, 2nd ed. W.H. Freeman and Company, NY, 859 p.

Appendix 1

The mean density for each cruise or stratum was estimated by the Sette-Ahlstrom method:

$$\bar{N} = \frac{\sum_i^n A_i \cdot N_i}{A} \qquad \text{(Richardson 1981)}$$

where $\bar{N}$ = mean number per 10 m^2,
A_i = area represented by station i (in units of 10 m^2),
N_i = number per 10 m^2 in sample i,

$A = \sum_i^n A_i$ = total area of survey or strata (in units of 10 m^2), and

n = the number of A_is in A.

Total abundance was estimated by $N = A \cdot \bar{N}$,

where N = total number in survey or strata.

The areas A_i are polygons as described in Richardson (1981). The variance of N was estimated using methods from probability sampling theory (Jessen 1978). The A_is may be different sizes, and one sampling unit (the water below 10 m^2 of surface area) is sampled in each A_i. Thus, the probability that a particular sampling unit is included in the survey depends on which A_i the sampling unit occurs.

$$P_{ij} = \frac{1}{A_i \cdot n}$$

where P_{ij} = probability that sampling unit j in A_i is selected in the survey.

This leads to the same estimate of $\bar{N}$ as given in Richardson (1981):

$$N_i = \frac{1}{A \cdot n} \cdot \sum_i^n \frac{N_i}{P_i} \qquad \text{(Jessen 1978, eq. 8.15)}$$

$$= \frac{1}{A \cdot n} \cdot \sum_i^n N_i \cdot A_i \cdot n$$

$$= \frac{\sum_i^n A_i \cdot N_i}{A}.$$

The estimate of the variance of mean density is

$$\hat{\mathrm{Var}}\,\bar{N} = \frac{1}{A^2 \cdot n \cdot (n-1)} \cdot \sum_i^n \left[\frac{N_i}{P_i} - \frac{1}{n} \cdot \sum_i^n \frac{N_i}{P_i}\right]^2 \qquad \text{(Jessen 1978, eq. 8.17)}$$

$$= \frac{1}{A^2 \cdot n \cdot (n-1)} \cdot \sum_i^n \left[N_i \cdot A_i \cdot n - \frac{1}{n} \cdot \sum_i^n N_i \cdot A_i \cdot n\right]^2$$

$$= \frac{n}{A^2 \cdot (n-1)} \cdot \sum_i^n \left[N_i \cdot A_i - \frac{A}{n} \cdot \bar{N}\right]^2.$$

And the variance of the total abundance is estimated by

$$\hat{\text{Var}}\, N = A^2 \cdot \hat{\text{Var}}\, \bar{N}.$$

Appendix 2

The centroid is simply the weighted bivariate mean of the sampled locations of the eggs or larvae. Its estimated value depends on where the samples were taken and the size of the catch. If the samples are not evenly or randomly spaced over the study area, then $(\bar{X}, \bar{Y})$ will be biased towards those areas with the highest sample density. This bias can be avoided by either grouping the individual samples into strata (sectors) as done here, or by modifying the computation of $(\bar{X}, \bar{Y})$ to account for unequal sample density as was done to estimate the mean and variance for the Sette-Ahlstrom method (see Appendix 1).

The rotation of the X and Y axes is specified by the slope of the principle axis, b_1 (Sokal and Rohlf 1981):

$$b_1 = \frac{\text{Cov}(X,Y)}{\lambda_1 - \text{Var}(X)},$$

where $$\text{Cov}(X,Y) = \frac{\sum_i N_i \cdot (X_i - \bar{X}) \cdot (Y_i - \bar{Y})}{\left(\sum_i N_i\right) - 1},$$

$$\lambda_1 = \text{the first latent root of the variance-covariance matrix of } X \text{ and } Y,$$

$$= 0.5 \cdot \left[\text{Var}(X) + \text{Var}(Y) + \sqrt{(\text{Var}(X) + \text{Var}(Y))^2 - 4 \cdot (\text{Var}(X) \cdot \text{Var}(Y) - \text{Cov}(X,Y)^2)}\,\right],$$

$$\text{Var}(X) = \frac{\sum_i N_i \cdot (X_i - \bar{X})^2}{\left(\sum_i N_i\right) - 1}, \text{ and}$$

$$\text{Var}(Y) = \frac{\sum_i N_i \cdot (Y_i - \bar{Y})^2}{\left(\sum_i N_i\right) - 1}.$$

The ellipse about the centroid is specified by the standard deviations along the rotated axes. The standard deviation in the direction of the major axis is equal to λ_1 as defined above. The standard deviation in the direction of the minor axis is equal to λ_2, which is the second latent root of the variance-covariance matrix of X and Y:

$$\lambda_2 = \text{Var}(X) + \text{Var}(Y) - \lambda_1.$$

Sokal and Rohlf (1981, box 15.5) give a formula for an ellipse of this shape but of a different size:

$$\text{Var}(Y) \cdot (X - \bar{X})^2 - 2\,\text{Cov}(X,Y) \cdot (Y - \bar{Y}) \cdot (X - \bar{X}) + \text{Var}(X) \cdot (Y - \bar{Y})^2 = C.$$

By setting C to the appropriate value, this formula can define the ellipse as specified above and shown in Appendix Figure 1. The value for C is derived from the formula for the point (X,Y) given in Sokal and Rohlf (1981, box 15.5):

$$X = \bar{X} + \sqrt{\frac{C}{\lambda_2 \cdot (1 + b_1{}^2)}} \qquad \text{and} \qquad Y = \bar{Y} + b_1 \cdot (X - \bar{X}).$$

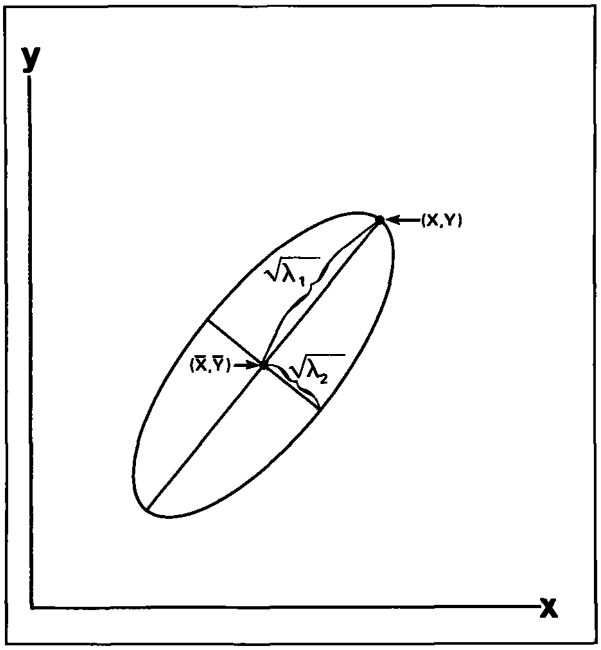

Appendix Figure 1
Ellipse with the center at $(\bar{X}, \bar{Y})$ and the major and minor axes each two standard deviations long.

The criterion that the length of the major axis is $2 \cdot \lambda_1$ implies that

$$\lambda_1 = (X - \bar{X})^2 + (Y - \bar{Y})^2$$

based on the Pythagorean theorem. By substituting in the formulas for X and Y given above, this formula can be rewritten as

$$\lambda_1 = \frac{C}{\lambda_2 \cdot (1 + b_1^2)} + \frac{b_1^2 \cdot C}{\lambda_2 \cdot (1 + b_1^2)} = \frac{C}{\lambda_2},$$

solving for C:

$$C = \lambda_1 \cdot \lambda_2 .$$

Thus the equation for the ellipse is

$$\mathrm{Var}(Y) \cdot (X - X)^2 - 2\,\mathrm{Cov}(X,Y) \cdot (Y - Y) \cdot (X - X) + \mathrm{Var}(X) \cdot (Y - Y)^2 = \lambda_1 \cdot \lambda_2 .$$

This ellipse is estimated by substituting the estimated values for the variances, covariance, means, and latent roots.

No distributional assumptions are needed to estimate the centroid, the slope of the principal axis, or the shape of the ellipse. The centroid is the standard measure of central tendency and is valid as long as the stations represent a valid sample of the survey area. The slope of the principal axis is defined by the line that minimizes the sum of the squared perpendicular distances between the data and the line. The size and shape of the ellipse are set by the variance of the data about the centroid. The ellipse is simply a two-dimensional version of a mean with standard error bars.

In the univariate case, the mean and standard error provide information about the location of the data's center of gravity and the amount of dispersion about that center, no matter what probability function the data come from (Shuster 1982). However, if the data are from a normal distribution, a confidence interval may be computed directly from the mean and standard error. If the data are from a bimodal or skewed distribution, the mean and standard error are still valid, but viewing the mean with standard error bars can give the false impression that the data are distributed symmetrically about the mean, when in fact the confidence interval would be asymmetrical if the data are asymmetrical.

Similarly, caution should be employed in interpreting the centroid and ellipse. No matter what probability function describes the spatial distribution of the eggs and larvae, the centroid is the measure of central tendency and the ellipse shows the orientation of the data and the amount of dispersion along the two axes. However, the ellipse can only be considered a contour or an "equal frequency ellipse" about the centroid if the data are from a bivariate normal distribution. In this case the proportion of the population expected to be enclosed by the ellipse may be estimated as follows.

Sokal and Rohlf (1981) state that if

$$C = \frac{\lambda_1 \cdot \lambda_2 \cdot (n-1) \cdot 2}{(n-2)} \cdot F_{\alpha[2,n-2]}$$

then the ellipse is expected to enclose $100 \cdot (1-\alpha)\%$ of the observations.

The α that corresponds to the ellipse used in this study can be determined by finding the value for α such that

$$\lambda_1 \cdot \lambda_2 = C = \frac{\lambda_1 \cdot \lambda_2 \cdot (n-1) \cdot 2}{(n-2)} \cdot F_{\alpha[2,n-2]},$$

which can be rewritten as

$$F_{\alpha[2,n-2]} = \frac{(n-2)}{(n-1) \cdot 2}.$$

If n is very large, then $(n-2)/(n-1)$ is close to 1 and

$$F_{\alpha[2,\infty]} \sim \frac{1}{2}$$

which corresponds to $\alpha = 0.6065$. Thus the ellipse is expected to enclose approximately 40% of the observations.

Appendix 3

The usual stratified estimate of variance is

$$\hat{\mathrm{Var}}\ \bar{N}_h = \frac{\sum_i A_{hi}^2 \cdot \hat{\mathrm{Var}}\ \bar{N}_{hi}}{A_h^2} \qquad \text{(Jessen 1978)}$$

which may be rewritten as

$$\hat{\mathrm{Var}}\ \bar{N}_h = \frac{\sum_{i_+} A_{hi_+}^2 \cdot \hat{\mathrm{Var}}\ \bar{N}_{hi_+} + \sum_{i_0} A_{hi_0}^2 \cdot \hat{\mathrm{Var}}\ \bar{N}_{hi_0}}{A_h^2}.$$

where i_+ refers to sectors with at least 2 samples, and i_0 refers to sectors with 1 or 0 samples.

There are no data to estimate Var $\bar{N}_{hi_0}$ directly, so it is estimated with the average variance from sectors where there are at least two samples.

Let

$$\hat{\mathrm{Var}}\ \bar{N}_{hi_0} = \frac{\sum_{i_+} A_{hi_+}^2 \cdot \hat{\mathrm{Var}}\ \bar{N}_{hi_+}}{\left(\sum_{i_+} A_{hi_+}\right)^2}, \text{ for all } i_0.$$

This estimate of Var $\bar{N}_{hi_0}$ is substituted back into the formula estimating Var $\bar{N}_h$, giving

$$\hat{\mathrm{Var}}\ \bar{N}_h = \frac{\sum_{i_+} A_{hi_+}^2 \cdot \hat{\mathrm{Var}}\ \bar{N}_{hi_+} + \sum_{i_0} A_{hi_0}^2 \cdot \dfrac{\sum_{i_+} A_{hi_+}^2 \cdot \hat{\mathrm{Var}}\ \bar{N}_{hi_+}}{\left(\sum_{i_+} A_{hi_+}\right)^2}}{A_h^2}$$

which simplifies to

$$\hat{\mathrm{Var}}\ \bar{N}_h = \frac{\sum_{i_+} A_{hi_+}^2 \cdot \hat{\mathrm{Var}}\ \bar{N}_{hi_+}}{A_h^2} \cdot \left[1 + \frac{\sum_{i_0} A_{hi_0}^2}{\left(\sum_{i_+} A_{hi_+}\right)^2}\right].$$